

Cite this: *Dalton Trans.*, 2019, **48**, 15121Received 20th July 2019,
Accepted 16th September 2019

DOI: 10.1039/c9dt02980j

rsc.li/dalton

Multi-color electrochromism from coordination nanosheets based on a terpyridine-Fe(II) complex†

Yu Kuai,^a Weijun Li,^a  Yujie Dong,^{*a} Wai-Yeung Wong,^b  Shuanma Yan,^a Yuyu Dai^a and Cheng Zhang^a 

A metal complex nanosheet was synthesized by the liquid–liquid interface self-assembly method from a star-shaped ligand of tris[4-(4'-2,2':6',2''-terpyridyl)-phenyl]amine in organic solvents and metal ion Fe(II) in water solution. The as-prepared nanosheet possessed excessively smooth morphology with a thickness of hundreds of nanometers. Adhering to an ITO glass, the nanosheet showed noticeable electrochromism from purplish red at 0 V to orange-yellow at 1.4 V and green at 1.6 V. Besides, the nanosheet exhibited outstanding stability with the optical contrast maintained at almost 100% of its original electrochemical activity over 500 cycles. The liquid–liquid interface self-assembly method was proven to be promising to prepare a polymeric metal complex for potential electrochromic applications.

Introduction

Electrochromic materials have been investigated extensively in the past decades due to their important potential applications in flat panel displays, smart windows, reflecting mirrors, enzymatic skin patches, and so on.^{1–9} In comparison with inorganic compounds,^{10–13} conjugated polymers possess plentiful and variable colors as well as fast color switching times and thus have attracted increasing attention in the current electrochromic research.^{14–18} However, the relatively poor electrochromic stability of most of the conjugated polymers has become a key critical defect for their future applications.¹⁹ Metal complexes have more stable electrochromic properties, and their electrochromic properties are tunable *via* changing the metals and ligands, which make the polymeric metal complexes capable of acting as promising electrochromic materials for future practical applications.^{20–24}

The polymeric electrochromic films are usually prepared by electropolymerization or spin-coating on an ITO glass. Recently, coordination nanosheets, *i.e.*, a class of two-dimensional (2D) materials featuring metal complex motifs were utilized by Nishihara and co-workers as electrochromic films.^{25–29}

These nanosheets were produced by liquid–liquid interfacial synthesis with an aqueous solution of metal ions and an organic solution of ligands. Taking advantage of the flexibility in ligand design and variety of metal ions, the desired polymeric metal complexes could be easily achieved as coordination nanosheets by self-assembly from a liquid–liquid interface.

2,2':6',2''-Terpyridine has been widely investigated as a ligand for d-block metal ions owing to its strong electron affinity; this moiety can be used to prepare highly stable complexes, supramolecular coordination compounds or polymers with interesting optical, electronic, and magnetic properties.^{29,31–33} With these characteristics, it has also been applied in the construction of coordination nanosheets.^{34–36}

Recently, we reported a star-shaped thiophene derivative (TPABT) consisting of one central core of triphenylamine and three arms of bithiophene and demonstrated the multi-color electrochromism of pTPABT derived from the oxidative states of the triphenylamine and quaterthiophene groups.¹⁶ In this work, we designed and synthesized a star-shaped molecule tris[4-(4'-2,2':6',2''-terpyridyl)-phenyl]amine (TPA-YPY) with triphenylamine as the central core and 2,2':6',2''-terpyridine as the peripheral arms (Fig. 1), aiming to achieve multiple electrochromic colors. We used the liquid–liquid interface self-assembly method (Fig. 2b) to obtain the terpyridine-Fe(II) complex nanosheets, which were generated at the interface between the dichloromethane (DCM) solution of TPA-TPY and the aqueous solution of Fe(BF₄)₂. After applying different voltages, multi-color electrochromism in the electrolyte solution containing a three-compartment system was observed for the obtained nanosheet film, which showed excellent electrochromic stability.

^aState Key Laboratory Breeding Base of Green Chemistry Synthesis Technology, College of Chemical Engineering, Zhejiang University of Technology, Hangzhou 310014, P. R. China. E-mail: dongyujie@zjut.edu.cn, czhang@zjut.edu.cn

^bDepartment of Applied Biology & Chemical Technology, The Hong Kong Polytechnic University, Hung Hom, Hong Kong, P. R. China.

E-mail: wai-yeung.wong@polyu.edu.hk

† Electronic supplementary information (ESI) available. See DOI: 10.1039/c9dt02980j

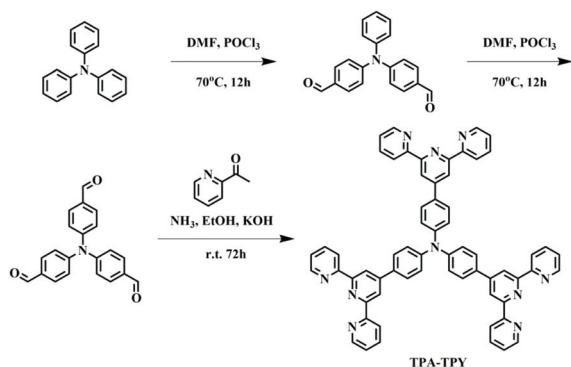


Fig. 1 The synthesis route of TPA-TPY.

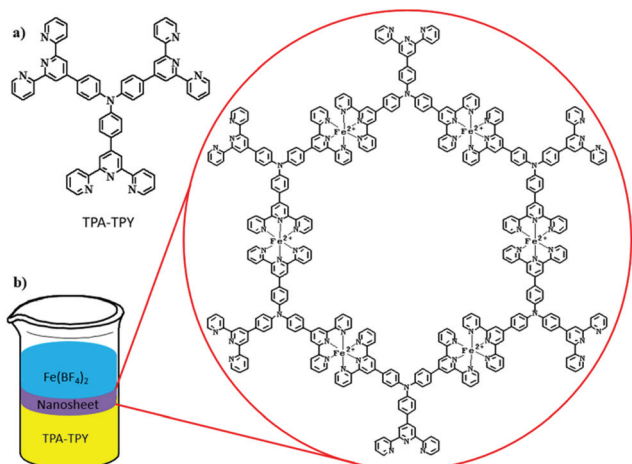


Fig. 2 (a) The chemical structure of ligand TPA-TPY. (b) The liquid-liquid interface self-assembly method and the chemical structure of the terpyridine-Fe(II) complex nanosheet.

lity with optical contrast remaining nearly unchanged after 500 cycles. Furthermore, a solid-state electrochromic device using the terpyridine-Fe(II) complex nanosheet as the electrochromic layer was fabricated to simulate practical applications.

Experimental

Materials and instrumentation

Reagents and solvents used in the synthesis and characterization were purchased from J&K, Aladdin and Energy Chemical, and used without further purification.

SEM was carried out with Nova NANOSEM 450. The electrochemical properties and long-term stability measurements were performed in a three-compartment system containing 0.1 M Bu_4NClO_4 in acetonitrile solution as the electrolyte on a CHI660C electrochemical analyzer. UV-vis spectra, optical contrast and switching time measurements were recorded on a Shimadzu UV-1800 UV-vis spectrophotometer. The thickness

of nanosheets was measured with a DEKTAK-XT profilometer. NMR was carried out with ANANCE III(500M). MS was carried out with SOLANX 70 FT-MS.

Synthesis

Synthesis of bis(4-formylphenyl)phenylamine. First, 10 ml (0.10 mol) of phosphorus(v) oxychloride was added dropwise to 8.0 ml (0.10 mol) of *N,N*-dimethylformamide at 0 °C. After 10 min, the reaction mixture was curdled, and 2.0 g (8.2 mmol) of triphenylamine was added. The reaction mixture was heated up to 70 °C and stirred for 12 h. After cooling down, the reaction mixture was poured into 100 ml of water at 0 °C and extracted with dichloromethane. The organic phase was dried by magnesium sulfate and evaporated. The crude product was purified by column chromatography on a silica gel with ethyl acetate/hexane (1 : 3, v/v) to yield a yellow solid (1.6 g, 80%). ^1H NMR (400 MHz, CDCl_3) δ 9.92 (s, 2H), 7.80 (d, J = 8.7 Hz, 4H), 7.42 (t, J = 7.8 Hz, 2H), 7.29 (m, 1H), 7.21 (m, 6H). MALDI FT-ICR-MS (mass m/z): 302.1186 [M^+ + H].

Synthesis of tris(4-formylphenyl)amine. Ten ml (0.10 mol) of phosphorus(v) oxychloride was added dropwise to 8.0 ml (0.10 mol) of *N,N*-dimethylformamide at 0 °C. After 10 min, the reaction mixture was curdled, and 2.0 g (8.2 mmol) of bis(4-formylphenyl)phenylamine was added. The reaction mixture was heated up to 70 °C and stirred for 12 h. After cooling down, the reaction mixture was poured into 100 ml of water at 0 °C and extracted with dichloromethane. The organic phase was dried by magnesium sulfate and evaporated. The crude product was purified by column chromatography on a silica gel with ethyl acetate/hexane (1 : 4) to yield an orange-yellow solid (1.0 g, 50%). ^1H NMR (400 MHz, DMSO) δ 9.95 (s, 3H), 7.92 (d, J = 8.6 Hz, 6H), 7.29 (d, J = 8.5 Hz, 6H). MALDI FT-ICR-MS (mass m/z): 330.1143 [M^+ + H].

Synthesis of tris[4-(4'-2,2':6',2''-terpyridyl)-phenyl]amine (TPA-TPY). Tris(4-formylphenyl)amine (0.20 g 0.60 mmol) and 2-acetylpyridine (0.50 g, 4.1 mmol) were stirred in tetrahydrofuran (30 ml), followed by the addition of potassium hydroxide (0.50 g, 8.9 mmol) and ammonium hydroxide (30 ml). After stirring for 72 h at room temperature, the greyish-green solid was precipitated. The precipitate was filtered and washed using tetrahydrofuran and then, the crude product was purified by recrystallization to yield an orange solid (0.10 g, 17%). ^1H NMR (400 MHz, CDCl_3) δ 8.79 (s, 6H), 8.77 (d, J = 9.2 Hz, 6H), 8.71 (d, J = 7.8 Hz, 6H), 7.91 (m, 12H), 7.38 (m, 12H). MALDI-TOF MS (mass m/z): 940.5 [M^+ + H].

Synthesis of coordination nanosheet. A 0.10 mM solution of TPA-TPY was prepared by dissolving 0.93 mg (0.0010 mmol) TPA-TPY in 10 ml CH_2Cl_2 . The solution (2.0 ml) was poured into a beaker of 10 ml (the cross-sectional area is about 18.1 cm^2) and then, water (2.0 ml) was added to cover the organic phase to form the interface. Next, 2.0 ml of aqueous solution of $\text{Fe}(\text{BF}_4)_2 \cdot 6\text{H}_2\text{O}$ (50 mM) was added slowly into the aqueous phase. The film emerged at the interface after 3 days. Pure dichloromethane replacing the organic phase by an injector was the same as the aqueous phase replaced by pure water. The film was fished out by an indium tin oxide (ITO) glass.

Results and discussion

The star-shaped TPA-TPY molecule was synthesized according to a method reported in the literature.²⁹ The nanosheets were obtained at the liquid–liquid interface between the CH_2Cl_2 solution of TPA-TPY and aqueous $\text{Fe}(\text{BF}_4)_2$ and were deposited onto an ITO glass (Fig. 3a). The thickness of the nanosheets for the reaction time of 5 days was measured to be approximately 55 nm (Fig. 3b). Interestingly, we found that the exterior color of the nanosheets gradually deepened with the extension of the standing time, and their thickness increased to ~ 70 nm after 6 days (Fig. S8†), ~ 90 nm after 7 days (Fig. S8†) and ~ 105 nm after 8 days (Fig. S8†). When we measured their UV-vis absorption spectra, all of the nanosheets with different thicknesses displayed similar characteristics with two typical absorption bands at ~ 400 nm and 580 nm (Fig. S1†). The results were consistent with those of the reported Fe^{2+} -terpyridyl coordination compounds,³⁰ indicating the successful preparation of the nanosheets through the self-assembly of Fe^{2+} metal ions and the TPA-TPY ligand molecule. The IR spectrum (Fig. S4†) shows that the peak at 1583 cm^{-1} , which belongs to the C=C stretching vibration of TPA-TPY, shifts to 1594 cm^{-1} for the nanosheet, indicating that the terpyridyl ligand coordinated to the metal ions. In addition, the broad peak around 1100 cm^{-1} should be attributed to BF_4^- .³⁰

We also used scanning electron microscopy (SEM) to evaluate the morphology of the nanosheets and found that the obtained nanosheets exhibited excessively smooth surface morphology (Fig. 4a). As shown in Fig. 4b and c, the obvious multi-layer sheet structure from the edge of the nanosheets indicates their layer growth model, which results in increased thickness with a static standing time. Energy dispersive spectroscopy (EDS) showed that the atomic percentages of N and Fe were 2.37% and 0.46%, respectively (Table S1†). The calculated ratio of N/Fe (5.2/1) was close to the ideal ratio of 6.6/1 in the metal complex structure of the nanosheets (Fig. 2b), further indicating that the obtained nanosheets self-assembled through the coordination between metal ions Fe^{2+} and the ligand molecule TPA-TPY.

Cyclic voltammetry of the nanosheets (8 days about 105 nm) on the ITO glass was carried out in a solution of acetonitrile with 0.1 M Bu_4NClO_4 as the electrolyte, and the

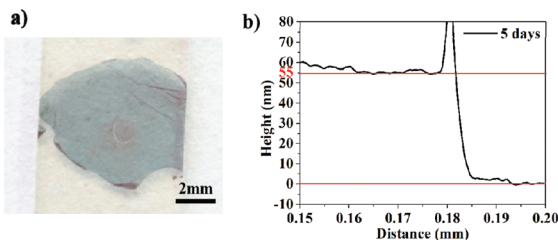


Fig. 3 (a) The nanosheet deposited onto ITO glass from the liquid–liquid interface between 0.1 mM TPA-TPY in CH_2Cl_2 and 50 mM aqueous $\text{Fe}(\text{BF}_4)_2$. (b) The thickness of the nanosheet with the reaction time for 5 days.

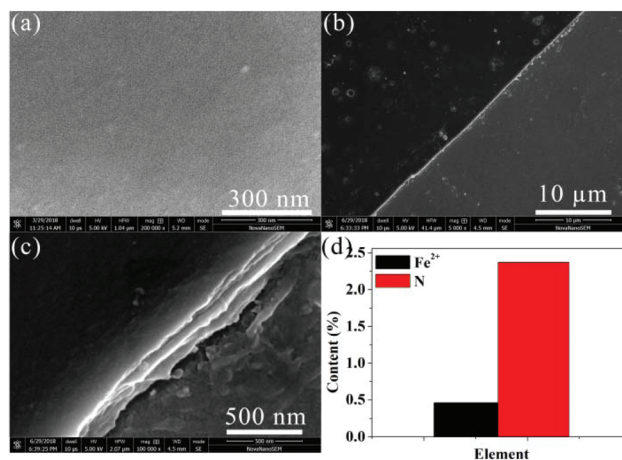


Fig. 4 The SEM images of body (a) and edge (b and c) of the nanosheet on ITO glass. (d) The histogram of EDS by contrasting N and Fe.

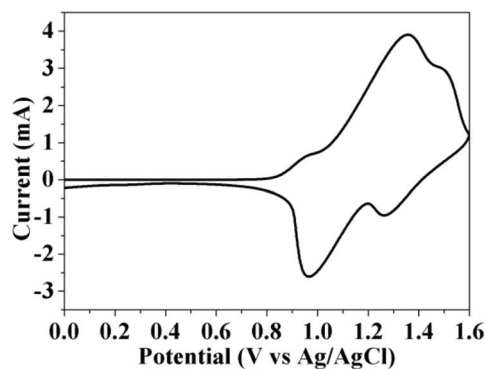


Fig. 5 Cycle voltammogram curve of the nanosheet.

applied voltage was set within 0–1.6 V at a scanning rate of 0.1 V s^{-1} . As shown in Fig. 5, there are two obvious reversible redox peaks with the oxidation peaks at 1.35 V and 1.49 V and the corresponding reduction peaks at 0.97 V and 1.27 V. Moreover, there is a weak oxidation peak under ~ 0.95 V, which is assigned to the doped or adhered TPA-TPY molecules according to the measured CV curves at the same experimental conditions (Fig. S2†). Considering the molecular structure of the nanosheets and the results reported in the literature, the two main redox peaks should be derived from the oxidation/reduction behaviors of coordinated $\text{Fe}(\text{n})$ -terpyridine (1.35/0.97 V) and central triphenylamine group (1.49/1.27 V), which might result in multi-color electrochromism for the nanosheets.

The electrochromic properties of the nanosheets were measured by a spectroelectrochemical experiment in a 0.1 M tetrabutylammonium hexafluorophosphate (TBAP)/acetonitrile solution. As shown in Fig. 6, the nanosheet displays a purplish red color with the maximum absorption peak at 580 nm at its neutral state under 0 V. In comparison with the result for its ligand TPA-TPY (375 nm in Fig. S3†), the large redshift of nearly 50 nm of the nanosheet should be mainly attributed to

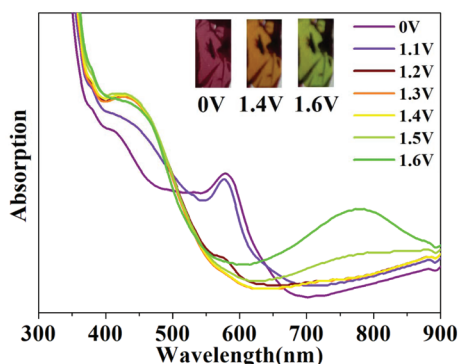


Fig. 6 UV-vis spectra of the nanosheet with applied potential from 0 V to 1.6 V in a solution of acetonitrile containing 0.1 M Bu_4NClO_4 . Inset: The color of nanosheet ($\sim 1.1 \text{ cm}^2$) with applied potentials at 0 V, 1.4 V and 1.6 V.

the metal-to-ligand charge transfer (MLCT) band of the coordinated Fe(II) -terpyridine group.³⁰ When the applied potentials were changed gradually from 0 V to 1.4 V, the absorbance at 580 nm decreased and even disappeared at last. At the same time, the absorbance at 421 nm rose gradually, which was accompanied by a color change from purplish red to orange-yellow. This transformation of the absorbance spectra was very similar to that of the reported coordinated Fe(II) -terpyridine group, indicating that the redox peak at 1.35/0.97 V should be attributed to the oxidation/reduction of the coordinated Fe(II) -terpyridine group in our nanosheets. By further enhancing the applied potential on the nanosheets from 1.4 V to 1.6 V, a new peak with λ_{max} at $\sim 780 \text{ nm}$ emerged, which was accompanied by an additional color change from orange-yellow to green. According to the reported literature data, this absorption band was consistent with that of the oxidative triphenylamine group, demonstrating that the redox peak at 1.49/1.27 V should be from the oxidation/reduction of the triphenylamine group in the nanosheets. It is obvious that the redox activity of our nanosheets consisted of two oxidation/reduction processes from the coordinated Fe(II) -terpyridine and triphenylamine groups, respectively, and this endowed the nanosheets with a multi-color electrochromism behavior from purplish red to orange-yellow and green.

The optical contrast and switching time were also tested under a repeated step potential between 0 V and 1.4 V with a residence time of 5 s. As shown in Fig. 7, for the fabricated nanosheets (8 days, about 105 nm) monitored at 580 nm, the optical contrast is measured to be 22.3%. The switching time, which is defined as the time required to achieve 95% of the full switch of the transmittance or color, was estimated to be 0.5 s for coloring and 0.4 s for discoloring. The fast switching time of the nanosheets was close to the reported data of electrochromism for polymers and obviously superior to those of electrochromism for inorganic oxides. The switching times of the nanosheets with different thicknesses were also tested under a repeated step potential between 0 V and 1.4 V with a residence time of 5 s (Fig. S5 and S6†).

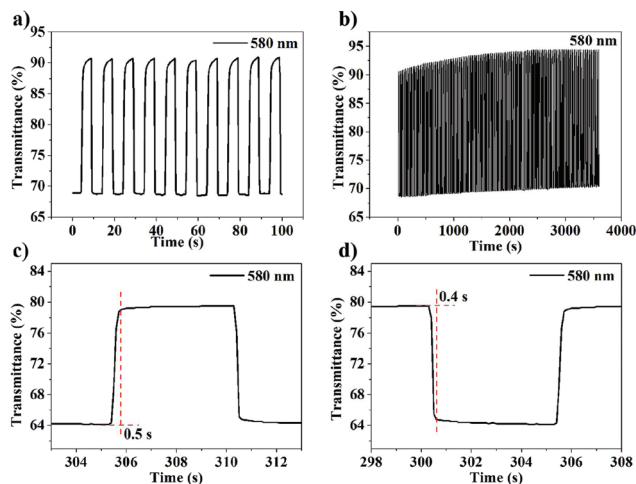


Fig. 7 (a) Optical contrast of the nanosheet switching electrified at 0 V and 1.4 V at 580 nm. (b) Stability of optical contrast of the nanosheet over 3500 s at 580 nm. (c) Response time of coloring. (d) Response time of discoloring.

The coloring times of nanosheets with the thicknesses of 55 nm (5 days), 70 nm (6 days), 91 nm (7 days) and 106 nm (8 days) were 0.7 (± 0.2) s, 0.5 (± 0.1) s, 0.6 (± 0.1) s and 0.6 (± 0.1) s, respectively; moreover, their discoloring times were 0.75 (± 0.25) s, 0.5 (± 0.1) s, 0.5 (± 0.1) s and 0.5 (± 0.1) s, respectively, which indicated that the switching time of the nanosheets is independent of the thickness (in the current thickness range of 55–106 nm). In addition, the coloration efficiency (CE) was calculated with the equation $\text{CE} = \Delta\text{OD}/Q_d$, and $\Delta\text{OD} = \log(T_c/T_b)$, where T_c is the transmittance of the oxidized state, T_b is the transmittance of the neutral state, and Q_d is the injected electronic charge in unit area. The CE values of the nanosheets of 5 days, 6 days, 7 days and 8 days were $12.84 \text{ cm}^2 \text{ C}^{-1}$, $29.29 \text{ cm}^2 \text{ C}^{-1}$, $73.61 \text{ cm}^2 \text{ C}^{-1}$ and $141.72 \text{ cm}^2 \text{ C}^{-1}$, respectively, which indicated that the CE value increased along with the increased thickness. Besides, the CE value is common to that of other electrochromic materials that have been reported.^{18,37} The nanosheets monitored at 580 nm also exhibited good stability with the optical contrast almost undiminished over 500 cycles, which corresponded to the redox behavior of the coordinated Fe(II) -terpyridine group. The green color electrochromism, which was observed at the higher applied potential of 1.6 V and should be attributed to the redox behavior of the central triphenylamine group, disappeared after several cycles with much worse electrochromic stability. This indicated that the coordinated Fe(II) -terpyridine complex part in our nanosheets possessed much better electrochromic stability than the organic triphenylamine group part. Though the optical contrast was not large enough, the fast switching time and excellent electrochromic stability made the metal complex capable of becoming a promising candidate material system for electrochromic displays.

As shown in Fig. 8(a), we fabricated a solid-state electrochromic device by using the nanosheet ($\sim 1.9 \text{ cm}^2$) as the electrochromic layer. The solidified electrolyte composed of

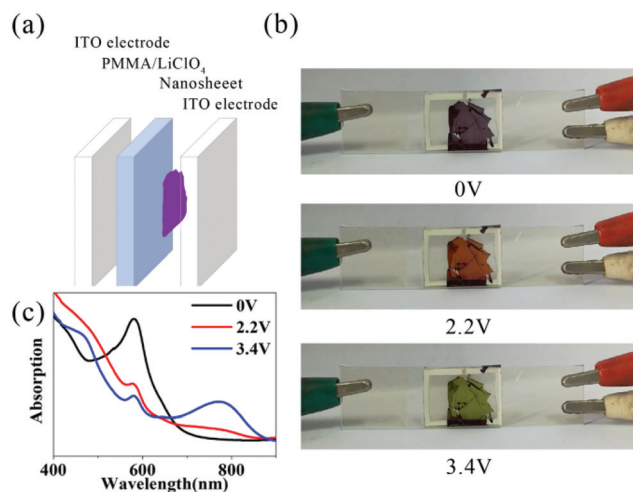


Fig. 8 (a) The structure of the solid-state device. (b) The color of the solid-state device at 0 V, 2.2 V and 3.4 V. (c) UV-vis spectrum of the solid-state device applied potential from 0 V to 3.4 V.

PMMA and LiClO_4 was sandwiched by two ITO glasses: one was blank ITO and the other one regarded as the working electrode was adhered to the nanosheet. The device color changed from purplish red to orange-yellow (Fig. 8b) as the applied potential was changed from 0 V to 2.2 V. At the same time, the absorbance at 580 nm decreased and that of 421 nm rose gradually, which was attributed to the MLCT band of the coordinated Fe(II) -terpyridine group (Fig. 8c). When the applied potential changed from 2.2 V to 3.4 V, the device color further changed from orange-yellow to green (Fig. 8b) with a new peak emerging at ~ 780 nm, which was assigned to the oxidation/reduction of the triphenylamine group (Fig. 8c). The changes in colors and UV-vis spectra were similar to those measured in the system of the electrochemical cell although the applied potential values were different. The switching time of the solid-state device was also tested under a repeated step potential between 0 V and 2.2 V with a residence time of 5 s (Fig. S7†). The switching time of the solid-state device was estimated to be 1 s for coloring and 0.9 s for discoloring, which indicated that the switching time of the nanosheet with the solid electrolyte was not different from that in the electrolyte solution. It is obvious that the liquid-liquid interface self-assembly method has been proven to be really practical for preparing a polymeric metal complex film for electrochromic applications.

Conclusions

We prepared coordination nanosheets based on a terpyridine- Fe(II) complex *via* the liquid-liquid interface self-assembly method. The nanosheets on an ITO glass exhibited an electrochromism behavior with a multi-color change from purplish red to orange-yellow and green with the gradually increasing voltage. Furthermore, the nanosheets showed a fast response

time with 2.1 s for coloring and 0.3 s for discoloring and could maintain excellent stability with almost invariable optical contrast over 500 cycles. This work demonstrates that the 2D polymeric metal complexes as nanosheets are capable of displaying multi-color electrochromism; moreover, their structural flexibility and variety provide prospects for a fast electrochromic switching speed close to that of polymers and excellent electrochromic stability potentially comparable to that of inorganic oxides.

Conflicts of interest

There are no conflicts to declare.

Acknowledgements

We are grateful for supports from projects funded by Zhejiang Provincial Natural Science Foundation of China (LY19E030006, LQ19E030016, LY17E030001), Natural Science Foundation of China (51603185, 51673174), Hong Kong Research Grants Council (PolyU 153051/17P) and The Hong Kong Polytechnic University (1-ZE1C). W.-Y. W. also thanks the support from the Endowed Professorship from Ms Clarea Au (847S).

Notes and references

- P. M. Beaujuge and J. R. Reynolds, *Chem. Rev.*, 2010, **110**, 268.
- A. C. Grimsdale, K. L. Chan, R. E. Martin, P. G. Jokisz and A. B. Holmes, *Chem. Rev.*, 2009, **109**, 897.
- A. L. Dyer, M. R. Craig, J. E. Babiarz, K. Kelly and J. R. Reynolds, *Macromolecules*, 2010, **43**, 4460.
- A. A. Argun, P. H. Aubert, B. C. Thompson, I. Schwendeman, C. L. Gaupp, J. Hwang, N. J. Pinto, D. B. Tanner, A. G. MacDiarmid and J. R. Reynolds, *Chem. Mater.*, 2004, **16**, 4401.
- V. K. Thakur, G. Q. Ding, J. Ma, P. S. Lee and X. H. Lu, *Adv. Mater.*, 2012, **24**, 4071.
- L. B. Groenendaal, G. Zotti, P. H. Aubert, S. M. Waybright and J. R. Reynolds, *Adv. Mater.*, 2003, **15**, 855.
- A. W. Lang, Y. Y. Li, M. D. Keersmaecher, D. E. Shen, A. M. Osterholm, L. Berglund and J. R. Reynolds, *ChemSusChem*, 2018, **11**, 854.
- L. R. Savagian, A. M. Österholm, D. E. Shen, D. T. Christiansen, M. Kuepfert and J. R. Reynolds, *Adv. Opt. Mater.*, 2018, **6**, 1800594.
- H. Kai, W. Suda, S. Yoshida and M. Nishizawa, *Biosens. Bioelectron.*, 2019, **123**, 108.
- X. J. Lv, J. W. Sun, B. Hu, M. Ouyang, Z. Y. Fu, Z. Y. Wang, G. F. Bian and C. Zhang, *Nanotechnology*, 2013, **24**, 1.
- Y. D. Shi, Y. Zhang, K. Tang, J. W. Cui, X. Shu, Y. Wang, J. Q. Liu, Y. Jiang, H. H. Tan and Y. C. Wu, *Chem. Eng. J.*, 2019, **355**, 942.

- 12 K. Hoshino, M. Okuma and K. Terashima, *J. Phys. Chem. C*, 2018, **122**, 22577.
- 13 D. Dong, W. W. Wang, A. Barnabe, L. Presmanes, A. Rougier, G. Dong, F. Zhang, H. Yu, Y. C. He and X. G. Diao, *Electrochim. Acta*, 2018, **267**, 277.
- 14 B. Schmatz, Z. B. Yuan, A. W. Lang, J. L. Hernandez, E. Reichmanis and J. R. Reynolds, *ACS Cent. Sci.*, 2017, **3**, 961.
- 15 W. J. Li, L. Chen, Y. Y. Pan, S. M. Yan, Y. Y. Dai, J. Liu, Y. Yu, X. X. Qu, Q. B. Song, M. Ouyang and C. Zhang, *J. Electrochem. Soc.*, 2017, **164**(4), E84.
- 16 Y. J. Dong, F. F. Luo, L. Chen, F. Y. Yuan, Y. J. Hou, W. J. Li, S. M. Yan, Y. Y. Dai, M. Ouyang and C. Zhang, *Phys. Chem. Chem. Phys.*, 2018, **20**, 12923.
- 17 S. M. Yan, W. J. Li, Y. Y. Dai, M. Ouyang, Y. J. Zhang and C. Zhang, *J. Electrochem. Soc.*, 2018, **165**(7), H342.
- 18 Q. Liang, X. J. Lv, M. Ouyang, A. Tameev, K. Katin, M. Maslov, Q. Bi, C. H. Huang, R. Zhu and C. Zhang, *ACS Appl. Mater. Interfaces*, 2018, **10**, 32404.
- 19 Y. Y. Dai, W. J. Li, X. X. Qu, J. Liu, S. M. Yan, M. Ouyang, X. J. Lv and C. Zhang, *Electrochim. Acta*, 2017, **229**, 271.
- 20 R. Sakamoto, K. Takada, X. S. Sun, T. Pal, T. Tsukamoto, E. J. H. Phua, A. Rapakousiou, K. Hoshiko and H. Nishihara, *Coord. Chem. Rev.*, 2016, **320–321**, 118.
- 21 H. Maeda, R. Sakamoto and H. Nishihara, *Coord. Chem. Rev.*, 2017, **346**, 139.
- 22 Y. W. Zhong, C. J. Yao and H. J. Nie, *Coord. Chem. Rev.*, 2013, **257**, 1357.
- 23 T. Mede, M. Jäger and U. S. Schubert, *Chem. Soc. Rev.*, 2018, **47**, 7577.
- 24 M. K. Bera, C. Chakraborty, U. Rana and M. Higuchi, *Macromol. Rapid Commun.*, 2018, **39**, 1800415.
- 25 R. Sakamoto, T. Yagi, K. Hoshiko, S. Kusaka, R. Matsuoka, H. Maeda, Z. Liu, Q. Liu, W. Y. Wong and H. Nishihara, *Angew. Chem.*, 2017, **129**, 3580.
- 26 R. Sakamoto, K. Hoshiko, Q. Liu, T. Yagi, T. Nagayama, S. Kusaka, M. Tsuchiya, Y. Kitagawa, W. Y. Wong and H. Nishihara, *Nat. Commun.*, 2015, **6**, 1.
- 27 T. Pal, T. Kambe, T. Kusamoto, M. L. Foo, R. Matsuoka, R. Sakamoto and H. Nishihara, *ChemPlusChem*, 2015, **80**, 1255.
- 28 A. Rapakousiou, R. Sakamoto, R. Shiotsuki, R. Matsuoka, U. Nakajima, T. Pal, R. Shimada, A. Hossain, H. Masunaga, S. Horike, Y. Kitagawa, S. Sasaki, K. Kato, T. Ozawa, D. Astruc and H. Nishihara, *Chem. – Eur. J.*, 2017, **23**, 8443.
- 29 T. Tsukamoto, K. Takada, R. Sakamoto, R. Matsuoka, R. Toyoda, H. Maeda, T. Yagi, M. Nishikawa, N. Shinjjo, S. Amano, T. Iokawa, N. Ishibashi, T. Oi, K. Kanayama, R. Kinugawa, Y. Koda, T. Komura, S. Nakajima, R. Fukuyama, W. X. Zhang, R. C. Han, W. Y. Liu, T. Tsubomura and H. Nishihara, *J. Am. Chem. Soc.*, 2017, **139**, 5359.
- 30 K. Takada, R. Sakamoto, S. T. Yi, S. Katagiri, T. Kambe and H. Nishihara, *J. Am. Chem. Soc.*, 2015, **137**, 4681.
- 31 T. Fatima, I. U. Din, A. Akbar, M. S. Anwar and M. N. Tahir, *J. Mol. Struct.*, 2019, **1184**, 462.
- 32 R. N. Soek, C. M. Ferreira, F. S. Santana, D. L. Hughes, G. Poneti, R. R. Ribeiro and F. S. Nunes, *J. Mol. Struct.*, 2019, **1184**, 254.
- 33 C. J. Yao, Y. W. Zhong, H. J. Nie, H. D. Abruna and J. N. Yao, *J. Am. Chem. Soc.*, 2011, **133**, 20720.
- 34 Y. Nishimori, H. Maeda, S. Katagiri, J. Sendo, M. Miyachi, R. Sakamoto, Y. Yamanoi and H. Nishihara, *Macromol. Symp.*, 2012, **317–318**, 276.
- 35 R. Sakamoto, Y. Ohirabaru, O. Matsuoka, H. Maeda, S. Katagiri and H. Nishihara, *Chem. Commun.*, 2013, **49**, 7108.
- 36 M. K. Bera, T. Mori, T. Yoshida, K. Ariga and M. Higuchi, *ACS Appl. Mater. Interfaces*, 2019, **11**, 11893.
- 37 D. C. Huang, J. T. Wu, Y. Z. Fan and G. S. Liou, *J. Mater. Chem. C*, 2017, **5**, 9370.